

STRATIGRAPHY, DISTRIBUTION OF ACTIVE LAYER AND DISCONTINUOUS PERMAFROST IN KANGIQSUALUJUAQ BASIN, NORTHERN QUEBEC

K. BEN-MILOUD and M.-K. SEGUIN

Department of Geology and Centre d'Études Nordiques, Université Laval Québec (Qc), Canada, G1K 7P4

Abstract

The hydrological basin is located to the southeast of Ungava Bay. This study is carried out to investigate the stratigraphy which is necessary for the understanding of the hydrological and thermal regimes of this basin. To establish the stratigraphic framework, surface geophysical surveys have been conducted. In addition, thermistor cables and piezometers are installed at three sites in order to obtain the parameters required for the hydrological and thermal investigations. The geophysical results are calibrated with drill hole information. The results of a ground probing radar profile are correlated with those of electrical soundings. This integrated approach facilitates the interpretation of geophysical soundings on uncalibrated sites and allows a better understanding of the stratigraphic sequences in marine sediments. Detailed transect surveys are conducted across the basin. These surveys indicate that permafrost covers 40% of the basin area. Its thickness, determined from geophysical surveys, varies from 2 to 20 m (average 11 m). The average permafrost thickness is similar in sand and gravel, till, and clayey silt deposits. On the test sites, the thickness of permafrost obtained from geophysical interpretation is compared with the extrapolated temperature profiles measured along drill holes. In addition, the depth extent of permafrost is correlated with snow cover thickness. Isotemperature sections and geoelectrical pseudo-sections indicate that permafrost is colder in stagnant waterlogged than in running water terrains. The results drawn from this study indicate the following: a) the permafrost stratigraphy is subdivided into cold and marginal parts and the percentage of the cold part represents 30% of the permafrost thickness, b) the permafrost disappears wherever snow cover exceeds 80 cm, c) discontinuous clayey silt lenses are observed underneath permafrost mounds, d) the best method to detect subpermafrost sediments, especially clayey silt lenses, is electrical resistivity sounding, e) the thermal regime of permafrost mounds is affected by the drainage pattern, and f) poor resolution is obtained from extrapolation technique where insufficient temperature data are available.

Résumé

Le bassin hydrologique est situé au sud est de la baie d'Ungava. Cette étude a été entreprise dans le but de détailler la stratigraphie nécessaire à la compréhension des régimes hydrologique et thermique du bassin. Pour ce faire, on a fait appel aux méthodes géophysiques de surface. De plus, on a installé des thermocâbles et des piézomètres sur trois sites afin de déterminer les paramètres requis pour cette étude. Les résultats géophysiques sont calibrés à partir de renseignements obtenus par des sondages mécaniques. Des transects d'observations ont été effectués en travers du bassin. Ces levés indiquent que le pergélisol s'étend sous 40% de la superficie du bassin. L'épaisseur du pergélisol déterminée par les levés géophysiques varie entre 2 et 20 m (moyenne: 11 m). L'épaisseur moyenne du pergélisol est sensiblement la même dans les divers dépôts rencontrés. Sur les trois sites, l'épaisseur du pergélisol estimée à l'aide des levés géophysiques est comparée aux profils thermiques extrapolés en profondeur. L'épaisseur du pergélisol est corrélée avec l'épaisseur du couvert de neige. Les sections géothermiques et les pseudo-sections géoélectriques démontrent que le pergélisol est plus froid dans les zones d'eau stagnante que d'eau courante. Les principaux résultats de cette recherche sont les suivants: a) la stratigraphie du pergélisol est divisée en deux secteurs, l'un froid et l'autre marginal; le premier représente 30% du total, b) le pergélisol disparaît lorsque le couvert de neige excède 80 cm, c) des lentilles discontinues de limon argileux sont présentes sous les buttes cryogènes, d) la méthode géophysique la plus efficace pour détecter les dépôts non consolidés sous la base du pergélisol est la résistivité électrique, e) le régime thermique des buttes pergélisolées est affecté par le patron de drainage, et f) la grande imprécision de détermination de la base du pergélisol à partir de l'extrapolation des températures saisonnières moyennes dépend surtout de la profondeur des trous de forage.

Introduction

In Canada, detailed studies of permafrost along with stratigraphy of unconsolidated deposits used to be limited by the availability of information from boreholes and natural sections. In the last two decades, an increasing use of

geophysical surveys has altered the situation in cryogenic environments (Seguin and Allard, 1987; Seguin *et al.*, 1989; Scott *et al.*, 1987). In Kangiqsualujuaq, northern Quebec, detailed surface and downhole geophysical studies related to permafrost were initiated in 1984 (Gahé *et al.*, 1987; Fournier *et al.*, 1987; Seguin and Allard, 1987; Allard and

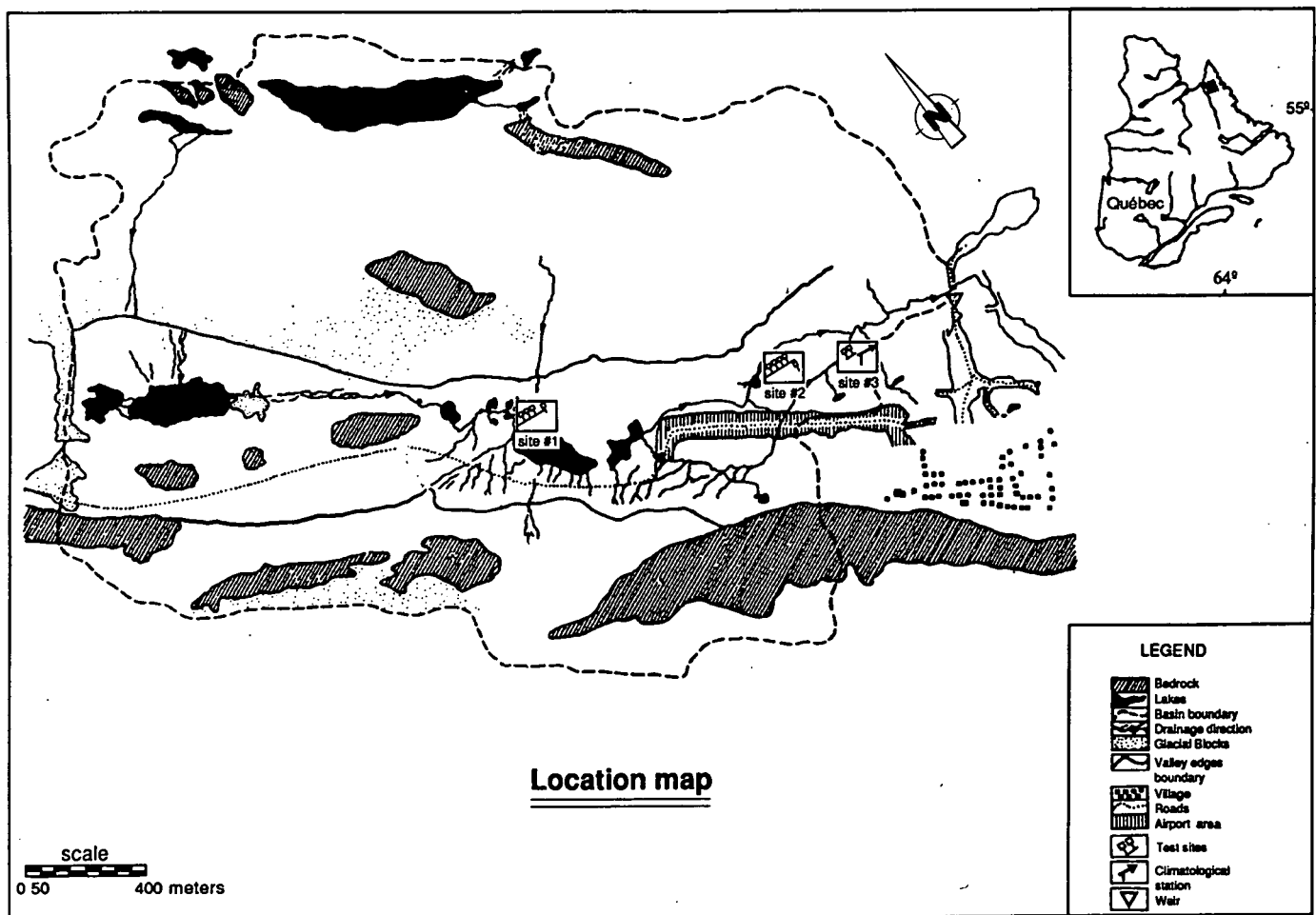


Figure 1. Location map

Seguin, 1987 and Seguin *et al.*, 1989). A variety of geomorphological units have been instrumented with multithermistor cables to study the characteristics of permafrost. Concurrently, these units have been investigated with a variety of geophysical methods including electrical resistivity soundings (ERS), induced polarization soundings (IPS), seismic refraction (SR) and recently ground probing radar (GPR) (Pilon *et al.*, in press). Additional geophysical surveys were carried out throughout the Kangiqsualujuaq basin and on three test sites within the basin in order to establish the stratigraphy at these sites and to extend this interpretation to the entire basin. In this paper, we present the results of different geophysical surveys as well as of thermal and hydrological investigations conducted within the basin and on test sites. The main objectives of this study are: 1) establishing the stratigraphy within the basin, 2) determining the best method suited to identify different stratigraphic units.

Description of the study area

The study basin lies close to the tree line (Payette, 1983) at 58°30' N and 65°50' W (Fig. 1) and near the border of discontinuous and continuous permafrost zones (Allard and Seguin, 1987). The basin is situated in a valley oriented NW-SE and flanked by steep bedrock scarps. The main annual air

temperature is -5.7°C and the annual precipitation amounts to 40 cm with a snow fraction of 45 to 50%. The elevations in this basin range from a maximum of 250 m on rocky ridges to a minimum of 10 m at the basin outlet. The basin is confined by an old shoreline to the NW and by George River to the SE. The rocky ridges and the old shoreline divert the drainage pattern towards George River. Most of the basin is covered by lichen (40-50%) and the rest by dwarf birch and black spruce on the basin edges. Carex and mosses occur in wet areas and scattered trees in a sheltered zone east of the basin. The basin is partly filled with glacial and marine deposits (Ben-Miloud *et al.*, in preparation). The till which has a sandy and occasionally silty matrix covers rocky hills and slopes. The marine deposits include sand and gravel in beaches and terraces as well as clayey silt. The bedrock consists of a grey biotite gneiss, part of an extensive metamorphic complex formed during Precambrian time (Taylor, 1974).

In order to achieve the above mentioned objectives, three sites were selected within the basin. These sites are representative of the predominant surface deposits in marine sand and of vegetation cover. Site #1, a cryogenic mound located in the centre of the basin, covers 900 m² and consists of fine to medium-grained sand and gravel. The water table is 10-15 cm below surface in the taliks. This site is almost flat and surface run-off is stagnant. Site #2, another mound

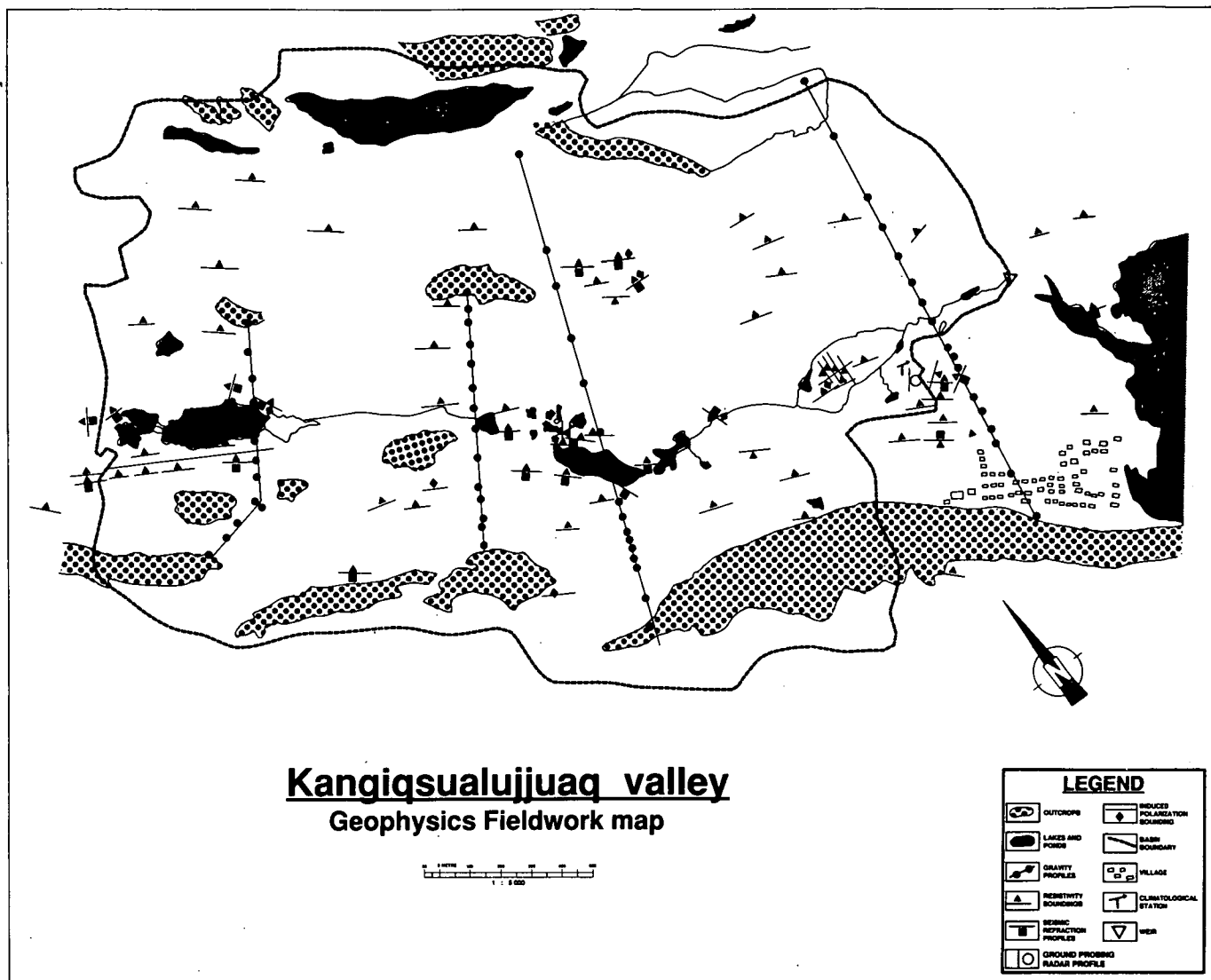


Figure 2. Surface geophysics field work map.

on the SE side of the basin, covers 1000 m² and consists of silty to fine-grained sand. The water table is 3-4 m below surface in the associated taliks and surface run-off is rapid. Site #3, a marine terrace on the far SE side of the basin, covers 1000 m² and consists of medium-grained sand and gravel. The water table is 3-4 m below surface in the local taliks and surface run-off is rapid.

Methodology

SURFACE GEOPHYSICAL METHODS

The logistics, data acquisition and processing of various geophysical surveys are briefly discussed. Further details on these methods are available in standard textbooks (Telford *et al.* 1976). Fig. 2 shows the location of 65 ERS, 12 IPS as well as 30 SR and one GPR profiles. These soundings and profiles are based on surface measurements and located in permafrost zones. The interpretation of ERS is made in the following manner. Apparent resistivity (ρ_a) is plotted against

current electrode half-spacings ($AB/2$) on 62.5 mm log-log paper. Increased electrode spacings represent larger depths of investigation. The observed results are matched with 2 and 3 layer master curves to obtain a preliminary model (Rijkswaterstaat, 1969). A computer program taking into account a more detailed multilayer model is used to improve the solution and to obtain a better fit of the observed and calculated results (Zodhy, 1975). The apparent resistivities and half-spacings are automatically converted into true resistivities (ρ) and thicknesses (t). The calculated (ρ) and (t) are subsequently grouped into realistic stratigraphic layers. Generally, a preliminary stratigraphic section is obtained with the aid of geomorphological and borehole information. To improve the accuracy of stratigraphy, surface geophysical interpretation is used. A typical example of ERS obtained on site #3 is shown in Fig. 3. The results are correlated with those obtained from GPR and SR profiles available on the same site (e.g. Fig. 3). The interpretation procedure of IPS is the same as for ERS. Chargeabilities are plotted against $AB/2$ to get a chargeability model which yields an independent solution of the parameters, i.e. thickness of active layer and permafrost as well as depth to bedrock.

**A typical example of ERS sounding and SR profile on site # 3
(ERS: 86-7-14-2 and SR: 86-6-26-3A)**

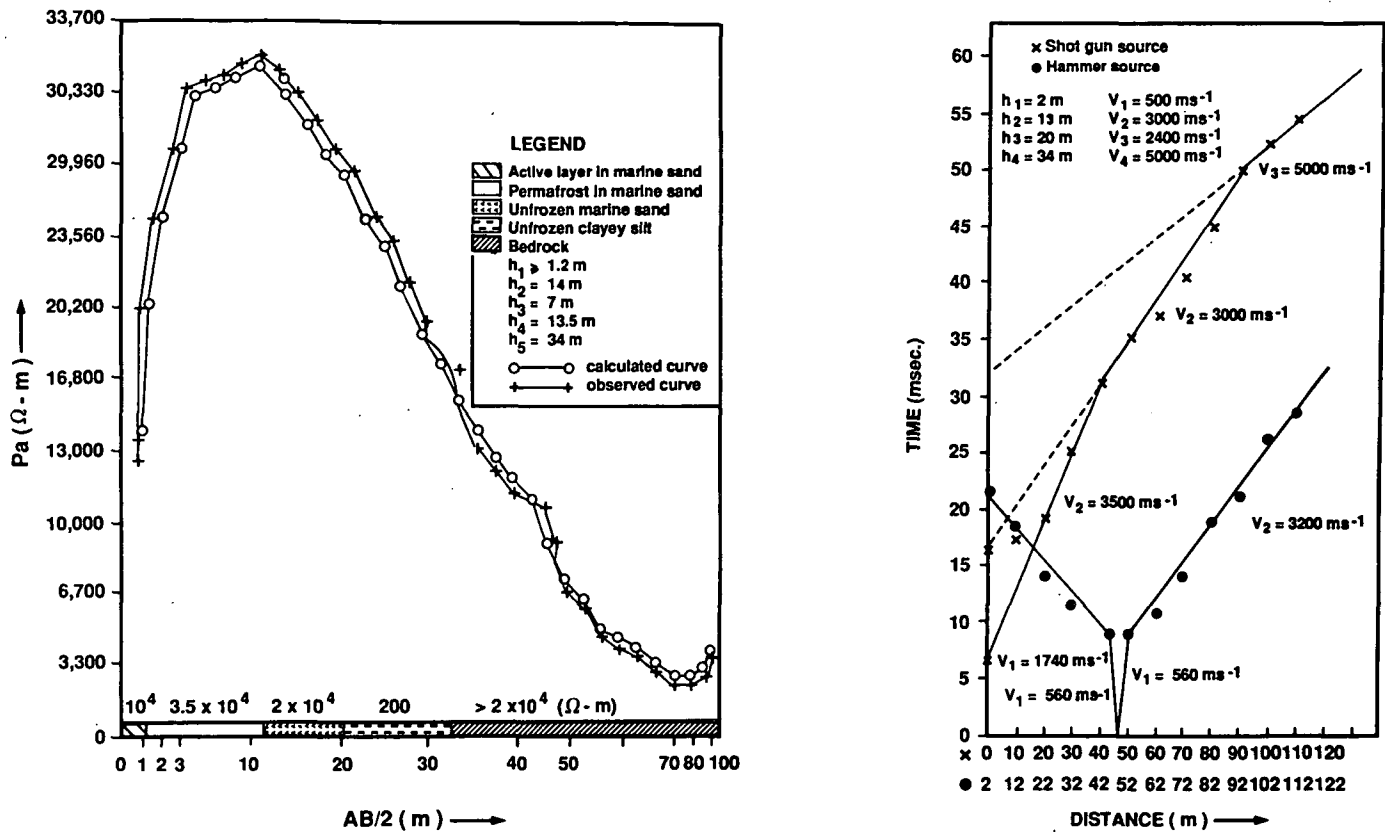


Figure 3. Electrical resistivity sounding (ERS) and seismic refraction (SR) profile on site #3.

Permafrost zones are characterized by high resistivities, low chargeabilities and high seismic velocities, these criterias are taken into account in the interpretation procedure. A typical example of IPS is illustrated in Ben-Miloud and Seguin (1987). IPS used in conjunction with a dipole-dipole array is particularly useful to obtain a two-dimensional image (pseudo-section) of permafrost in cryogenic mounds on sites #1 and #2. For this configuration, the spacing for each dipole set is 2 m. The spacings between the two dipoles are taken by steps of 2 m from 2 to 12 m. On a pseudo-section, values are plotted on the vertical axis at the intersection points of 45° lines drawn from surface and originating at mid-points of current and potential electrodes. The values of (ρ_a) and apparent chargeabilities (m_a) are plotted at points directly below the center of the electrodes spread. The depth of penetration increases with an expanding spread. Contours of equal ρ_a and m_a values are drawn on these pseudo-sections (Telford, 1976). A typical example of pseudo-sections on sites #1 and #2 is shown in Figs. 4 and 5. The results are interpreted in the form of sections making use of ρ_a and m_a contrasts. These sections are correlated and compared with both isotherm sections and other surface geophysical results gathered on the same sites. The interpretation and results of the GPR profile are presented by Pilon *et al.* (in press); this profile is located on site #3 (Fig. 2). In addition, the interpretations and results of the SR profiles are shown in Ben-Miloud and Seguin (1987). A typical example of SR profile obtained on Site #3 is shown in Fig. 3.

The confidence level placed on geophysical interpretations is controlled by drill hole information, correlation with the stratigraphy of natural and artificial cuts and the comparison of the results acquired with different geophysical methods (Seguin *et al.*, 1989). Generally, the relative error does not exceed 15%.

HYDROLOGICAL AND THERMAL TECHNIQUES

The installation of piezometers and thermistor cables in addition to field observations on the test sites are discussed in Ben-Miloud *et al.* (in preparation). Piezometers are installed on sites #1 and #2. These piezometers are installed in the taliks along the surface flow directions. At site #1, three piezometers are at depths of 4.71, 3.61 and 4.81 m. At site #2, five piezometers are at depths of 8.50, 8.0, 5.24, 6.30 and 8.90 m. Subsurface temperatures are measured along these piezometers using a single thermistor mounted on a portable cable which is lowered at 1 m intervals. Temperature readings and water levels are recorded once in the summer, fall and winter seasons. In addition, four permanent thermistor cables are installed in the frozen zone of sites #1 and #2 respectively and two others in site #3. The permanent thermistor cables are installed across the cryogenic mounds from one talik to the next on the other side of the mounds. The thermistors are spaced at 1 m interval. At site #1, the thermistor cables are drilled to depths

Pseudo-resistivity, chargeability and isotherm sections on site # 1 (25-07-1988)

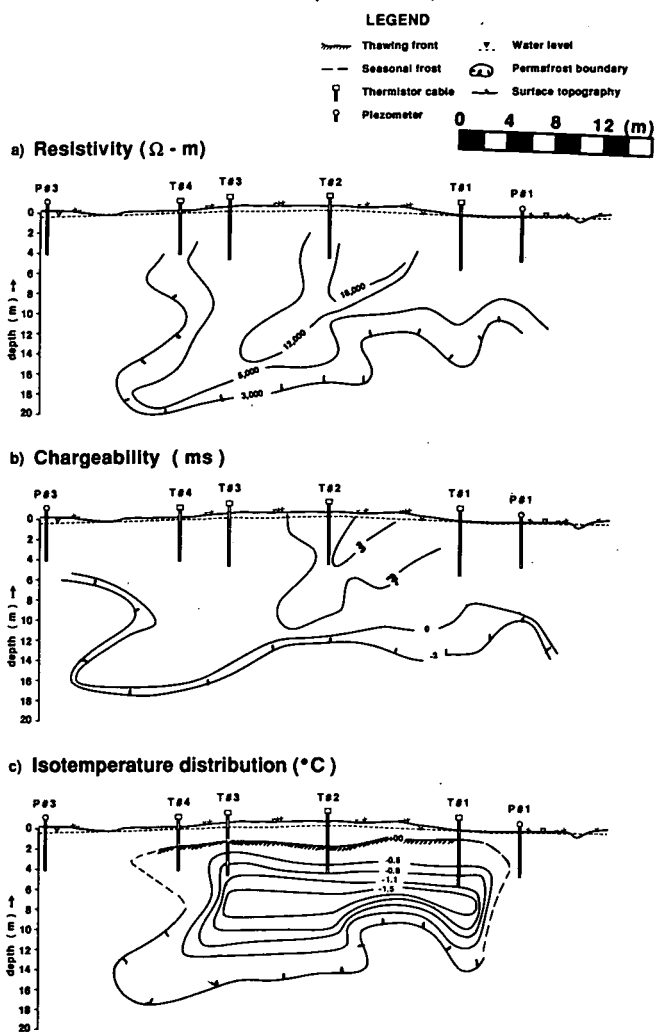


Figure 4. Pseudo-resistivity-chargeability distribution and isotherm sections on site #1.

ranging from 4 to 6 m. For site #2, the depths range from 6 to 9 m and for site #3 from 7 to 10 m. Fig. 6 shows the variations of temperature obtained from a cable in the centre of the mound and resistivity and chargeability on pseudo-sections as a function of depth. These temperature variations are correlated and compared with surface geophysical results obtained from the same sites and at the same period. Isotherm values were contoured on sites #1 and #2. Typical examples of isotherm sections are shown in Figs. 4 and 5. Temperature measurements are extrapolated to the 0°C isotherm in order to outline the base of permafrost (Figs. 7 and 8).

A straight line is fitted to the observed temperature-depth profiles. In reality, an exponentially decreasing function with depth should be used. For most of the observed temperatures with the exception of cases (b) and (c) on site #2 (Fig. 8), an insufficient number of temperatures is available to use exponential regression. Consequently, only a minimum depth to the base of permafrost is estimated. For

Pseudo-resistivity, chargeability and isotherm sections on site # 2 (25-07-1988)

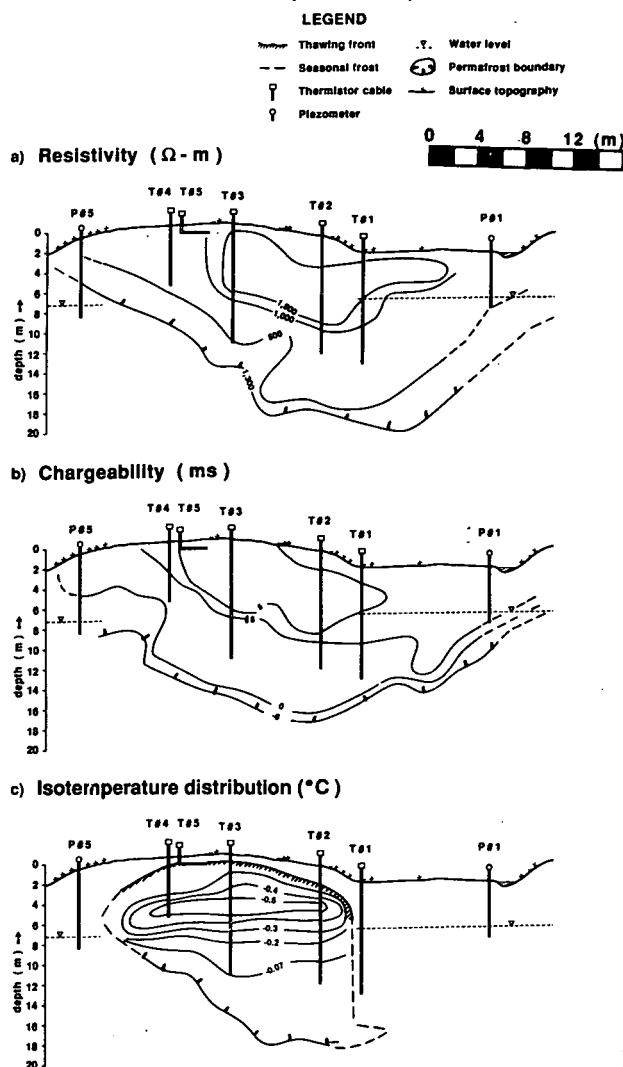


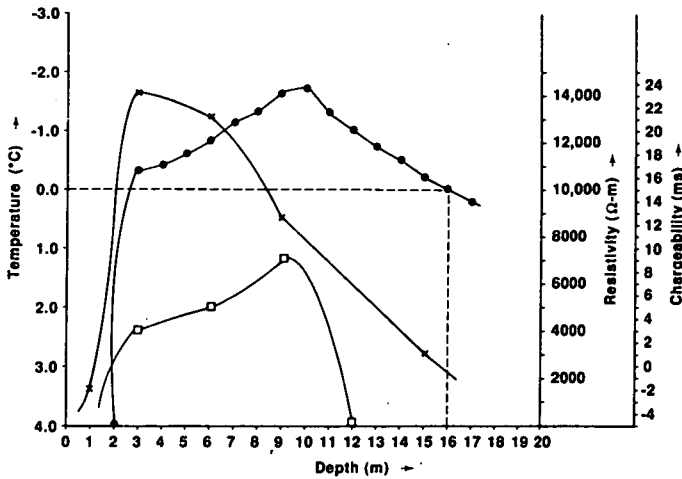
Figure 5. Pseudo-resistivity-chargeability distribution and isotherm sections on site #2.

thermistor cable T #3 (Fig. 8), an exponential regression lowers the base of permafrost by 1 m and for thermistor cable T #2 by 2 to 3 m.

The average seasonal temperatures produces a more linear function of temperature (T) with depth (d) than does the average for a specific season. This allows an approximate (minimum) estimate of the base of permafrost even if only a few (T-d) values are available. The use of depth as independent variable does not change the results. The extrapolation of temperature measurements at depths is carried out for the period of July and November 1987, March, July and October 1988 and March 1989. Average temperature values for the six seasons are plotted against depths on sites #1 and #2. The position for 0°C at the base of permafrost is outlined with the help of integrated geophysical interpretation and temperature results from deeper drill holes within the basin. In this area, the minimum temperature values of permafrost (cold part) during the

Temperature, resistivity and chargeability distribution vs depth on sites #1 & #2 (25-07-1988)

a) site #1 T#2 (Cable #2 Bas)



b) site #2 T#3 (Ben-Miloud #3)

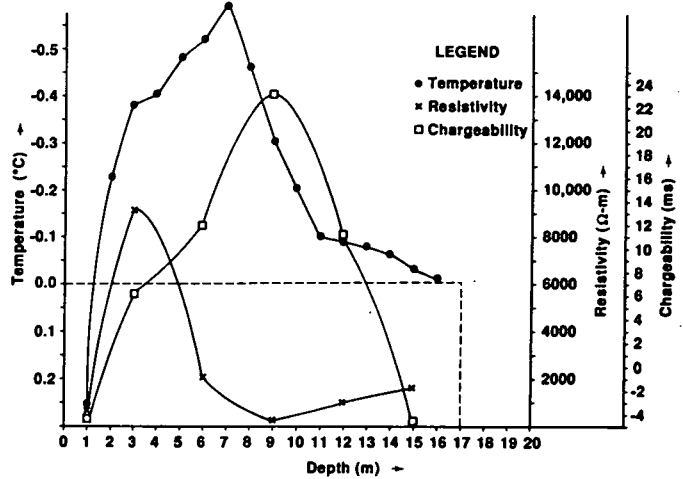
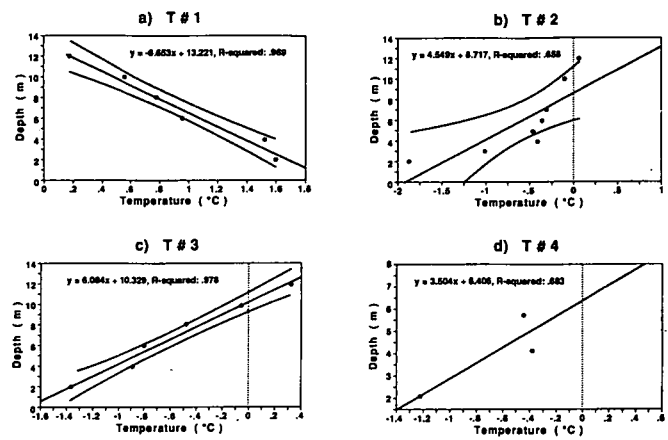
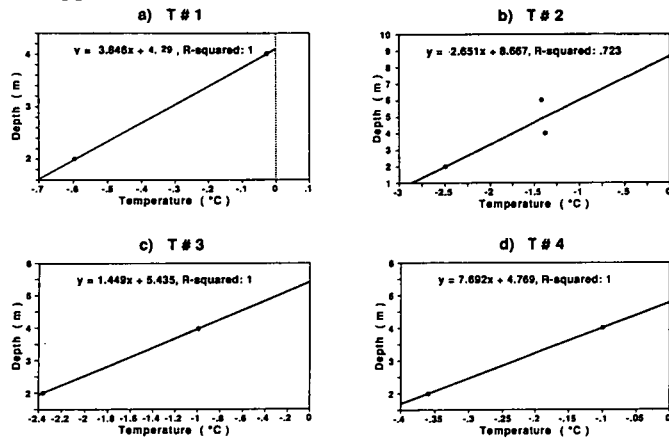


Figure 6. Temperature, resistivity and chargeability distribution vs depth on sites #1 and #2. Both resistivity and chargeability are apparent values.



Temperature extrapolation to obtain the base of permafrost on site #1

Figure 7. Extrapolated temperature measurements on site #1. Note that the depth is increased vertically on the Y-axis. The 0 m depth is not shown because the permafrost table is located slightly above the 2 m depth; in the active layer, temperature variations are too large to provide a seasonal temperature average.

Temperature extrapolation to obtain the base of permafrost on site #2

Figure 8. Extrapolated temperature measurements on site#2. The comments of Fig. 7 apply to Fig. 8.

summer season is located in the depth range: 4-7 m. The depth of one hole on site #1 yields an estimate of the minimum temperature values (-1.5°C). The results obtained from the extrapolation of temperature at depth and from surface geophysics are compared (Figs. 7 and 8).

SURFACE GEOPHYSICAL RESULTS

A comparison of the thickness of the stratigraphic units obtained from ERS, SR, GPR and temperature investigations is fairly good. The GPR profile provides a thickness of thaw front between 1.5 and 2 m, thicknesses of cold and marginal parts amounting to 6 and 12.5 to 15.5 m (the total thickness of permafrost ranges between 18.5 and 21.5 m). Similar results are obtained with other methods; however, SR and ERS yield the whole thickness of permafrost without distinction between the cold and marginal parts (13 and 14 m with SR and ERS respectively, Fig. 3). On the other hand, ERS give thicknesses of the unfrozen soil layer underneath the base of permafrost; these cannot be obtained with SR or GPR profiles. This is so because clayey silt material present in this site (site #3) causes velocity inversion problems for SR and attenuation of the electromagnetic signal for GPR. This leads to the fact that ERS is more reliable in such cases. Therefore, the entire thickness of permafrost at this site is 14 m. Figs. 6a

The procedures followed along the transect survey, the spacings of the observation points and maps obtained from this survey are provided in Ben-Miloud *et al.* (in preparation).

Results

Results are divided in two parts: surface geophysical data and field observations.

and b show that the cold and marginal parts of permafrost are 4 to 6 m and 10 to 12 m respectively. In addition, the resistivity and chargeability curves yield a rough estimate of the cold part of permafrost thickness (4–6 m). In this cold section, the electrical resistivity is maximum and the chargeability is low (e.g. Fig. 4). Figs. 4 and 5 show higher resistivity values in the pseudo-section of site #1 than in those of site #2. The contour lines are drawn according to the numerical values plotted in the pseudo-sections. The high resistivity values on site #1 are plunging to the SE direction. This means a thickening of permafrost towards this direction. The resistivity values (1.2×10^4 to $1.6 \times 10^4 \Omega\text{-m}$) are observed around thermistor cable T #2 and around the centre of the permafrost mound. Similar patterns are observed in the chargeability and temperature sections in which the high chargeability values are in the range of 3–7 ms whereas the lowest temperature value is -1.5°C . The temperature section shows that the thicker part of permafrost corresponding to the cold portion is confined between thermistor cables T #2 and T #3 (Fig. 4). On site #2, the high resistivity values in the pseudo-section are plunging to the NW direction. These high values range from 0.1×10^4 to $1.5 \times 10^4 \Omega\text{-m}$. Low chargeability values are in the range of 5–18 ms and the lowest temperature value is -0.5°C . This zone indicates the cold part of permafrost. The thicker part of permafrost observed on the temperature section is confined to the zone between T #2 and T #3. The permafrost thickness observed in these sections on sites #1 and #2 are in the order of 14–15 m and 12–14 m respectively. Similar results are obtained with ERS.

Even though the resistivity values on site #1 are higher than on site #2, the chargeability values are lower on site #1 than site #2. This is so because more unfrozen water is present in the upper part of permafrost (2–4 m) in site #2 than site #1. Fig. 7 shows that the base of permafrost on site #1 is 4, 8.5, 5.5 and 4.5 m as estimated from T #1, T #2, T #3 and T #4 respectively. The discrepancy (80%) between the thicknesses obtained from thermistor cables (Fig. 7) and that of surface geophysical methods is due to an insufficient number of temperature values required by the extrapolation technique and the shallow depth of boreholes. Thermistor cables T #1 and T #4 measure the shallower and warmer portion of permafrost in comparison with T #2 and T #3 located in the centre of the mound. Therefore, the thickness obtained from T #1 and T #4 does not represent the exact thickness of permafrost. Consequently, this thickness is not comparable with the thickness obtained from surface geophysical methods. Fig. 8 indicates that the base of permafrost on site #2 is 9, 10 and 6.5 m as estimated from T #2, T #3 and T #4 respectively. The thermistor cables T #4 and T #1 are located in the SE and NW edges of the permafrost mound while the others are located in the centre of the mound. Therefore, T #4 and T #1 represent the shallow part of permafrost. T #1 indicates that all temperature distributions are above 0°C and reach equilibrium close to 0°C at a depth of 12 to 13 m. In this case, T #1 does not yield the true permafrost thickness. The comparison of permafrost thicknesses obtained from T #2, T #3 and T #4 (Fig. 8) with that of surface geophysical data on site #2 is fairly good (25% of error). This results from the availability of a sufficient number of temperature data required for the

Stratigraphic cross-section obtained from surface geophysics and temperature data on site #3

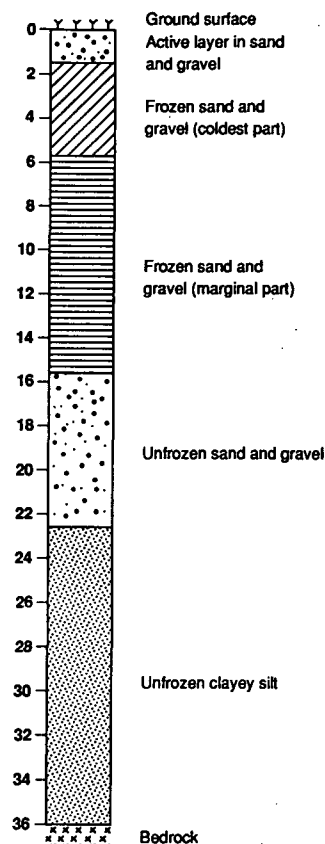


Figure 9. Typical stratigraphic cross-section on site #3

extrapolation at depth. Fig. 9 shows the stratigraphic cross-section obtained from the integrated results of surface geophysics and of the isotherm section on site #3. The stratigraphy is controlled by borehole observations down to a depth of 16 m as well as a man-made section (gravel pit) which is 20 m deep. The remaining part of the section is interpreted from surface geophysical results. The thickness of active layer, permafrost and depth to bedrock is 1.6, 14 and 36 m respectively. The thickness of the cold and of marginal parts of permafrost are 4.2 and 9.8 m.

FIELD OBSERVATION RESULTS

From the transect surveys mentioned previously, different maps are outlined. These maps represent surface deposits, soil types, snow cover and thaw front distribution. The surface deposits map includes the lateral distribution of permafrost, drainage pattern and vegetation types. A description of surface conditions and materials is needed to constrain the stratigraphy near the surface, the hydrological regime and lateral distribution of permafrost. The total area of the basin, of permafrost and that of rock outcrops determined from this map amounts to 6.0×10^6 , 2.4×10^6 and $0.56 \times 10^6 \text{ m}^2$ respectively. The surface criterias considered to estimate discontinuous permafrost patches are

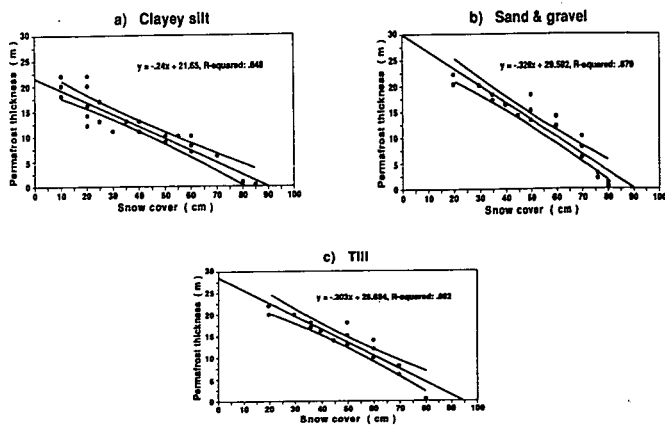


Figure 10. Overburden permafrost thickness vs snow cover thickness

mainly based on the occurrence of specific vegetation types (e.g. lichen cover), minimum thickness of snow cover (<80 cm) and scarcity of drainage patterns. The percentage of permafrost within the basin area is 40% or 49.5%. This last figure is determined when outcrops are considered to be frozen.

The snow cover distribution map matches very well with the physiography of the basin (i.e. the highest snow cover is noticed along depressions, stream flow, lakes and ponds, shrubby zones and the lee sides of cliff). The largest snow cover thickness (150-180 cm) is observed in shrubby zones located on the SE side of the basin and in depressions of streams and ponds. The smallest snow cover thickness (10-15 cm) is observed on the south and north-facing slopes as well as on elevated permafrost mounds. The average snow cover (60-70 cm) is observed along the basin bottom. Fig. 10 shows the relation between permafrost thickness obtained from surface geophysical results and the observed snow cover thickness. This diagram shows a decrease of permafrost thickness with increasing snow cover for the three major soil types; permafrost disappears when the snow cover exceeds 80 cm. The high values of the coefficients of determination (r^2) suggest that 85% of the variation in permafrost thickness can be explained by the linear regression with snow cover. The absence of permafrost is confirmed by both field observations and surface geophysics when the snow cover is larger than 80 cm. For snow cover smaller than 80 cm, field observations do not allow an estimate of permafrost thickness while surface geophysical methods do so. Fig. 11 illustrates the thaw front variations along the permafrost mounds within the test sites. On site #1, the average thaw front variations observed during June, August and October are 20, 90 and 150 cm respectively. On site #2, the average thaw front variations observed during the same period are 15, 100 and 150 cm. These results are confirmed with temperature data and with surface geophysical interpretation. As a result of the field observations from the transects and surface geophysical surveys, a typical section across the study basin is presented in Fig. 12. This cross-section shows the thickness of permafrost and the depth to bedrock which ranges from 6 to 20 m and from 0 to 45 m respectively. At an altitude greater than 70 m, exposed bedrock is frozen.

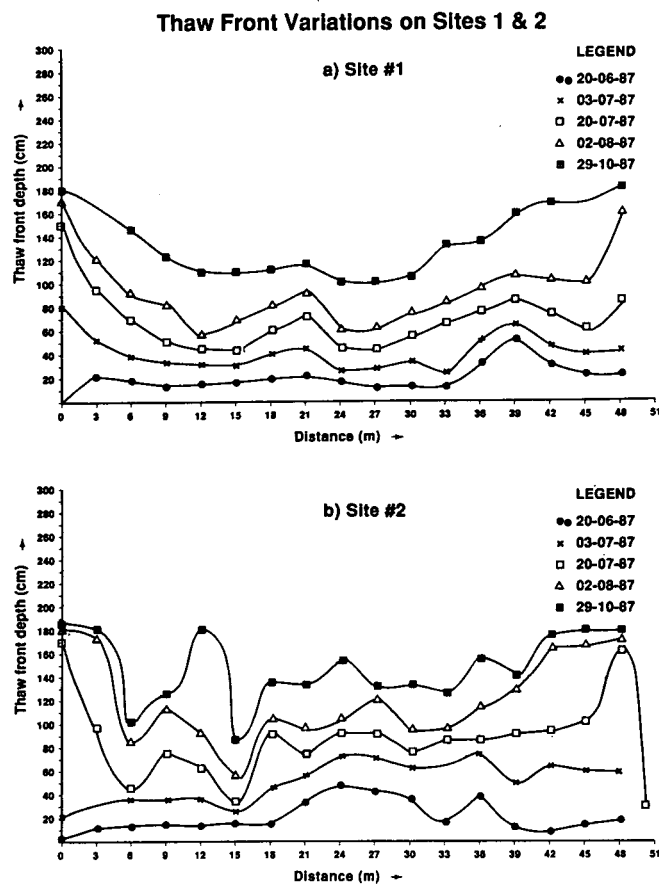


Figure 11. Thaw front variations on sites #1 and #2. Note that the depth is increasing vertically on the Y-axis.

Discussion

Updated investigations of stratigraphic sequences show that ERS is the most reliable geophysical method for permafrost detection. It allows in almost 100% of the cases the detection of unfrozen unconsolidated deposits confined between the permafrost base and bedrock. It yields a reliable estimate of their thicknesses. The relative error in thickness estimation ranges from 15-20% as verified by an increasing number of calibrations from drill holes and natural sections. However, ERS is not always the best tool to arrive at a detailed description of permafrost stratigraphy. The comparison of ERS with GPR and temperature data on site #3 indicates that the total thickness of permafrost is 14 m. The thickness of cold and of marginal parts of permafrost estimated are 4.2 and 9.8 m respectively. A confirmation of these results is presented in Figs. 4, 5 and 6 respectively. Therefore, for uncalibrated sites within the basin where ERS is the only surface geophysical method used and where no thermistor cables are available, the cold part of permafrost is estimated at 30% of its entire thickness.

Even though the surface and subsurface conditions, i.e. vegetation cover, soil type (including thermal conductivity) and snow cover, are the same on sites #1 and #2, site #1 is colder than site #2 (Figs. 4 and 5). This observation is witnessed by the higher resistivity and lower temperature values on site #1 than site #2. These differences may result

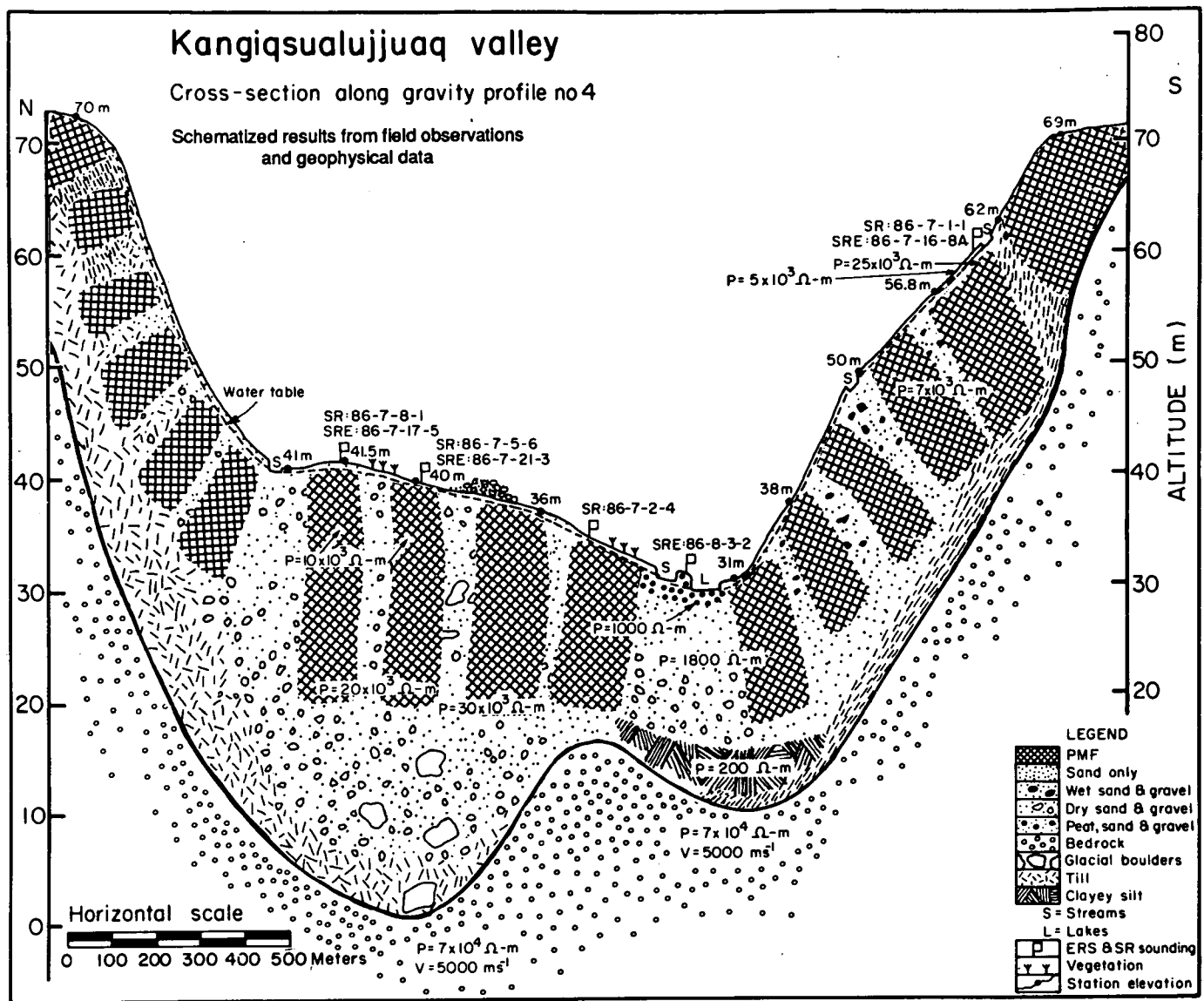


Figure 12. Schematic results from field observations and geophysical investigations across the study basin.

from different drainage patterns. On site #1, surface water is stagnant while on site #2, the surface water is running. Therefore, heat is added to site #2 by running water through convection while on site #1 heat convection is negligible.

Conclusions

The conclusions which can be drawn from this study are the following: the maximum depth of thaw front (active layer) for fine sand and clayey silt materials is 150 cm and this is observed at the end of October. Active layer thicknesses for other soil types is presented in a table form by Ben-Miloud *et al.* (in preparation). The thickness of the cold part of permafrost is 4-6 m while the underlying marginal part is 10-12 m. The percentage of cold and marginal parts of permafrost thickness are 30 to 70 % respectively. The best surface geophysical method giving a high resolution for the stratigraphy of all soil types at the

exclusion of dry sand and till is ERS. For a detailed description of permafrost stratigraphy, GPR is often more reliable in medium-to coarse-grained materials such as marine sand and till. The determination of the base of permafrost by extrapolation of temperature data to the 0°C isotherm is not useful when the thermistor cables are shallow. No permafrost is found when the snow cover exceeds 80 cm. The stagnant waterlogged site is colder than the running water site.

Acknowledgements

The authors gratefully acknowledge the financial support of the Centre d'Études Nordiques and grants from NSERC and FCAR. Thanks are due to C. Bouchard, G. Dionne, R. Fortier and R. Lévesque for their help in the field study. The valuable comments of Dr. M. Allard are gratefully acknowledged.

References

- ALLARD, M. & M.K. SEGUIN, 1987. Le pergélisol au Québec Nordique: Bilan et perspectives. *Géogr. phys. et Quat.*, 41:141-152.
- BEN-MILOUD, K. & M.K. SEGUIN, 1987. Solution of velocity inversion in seismic refraction surveys with the use of electrical methods in three types of terrains from the Kangiqsualujuaq Valley, Northern Quebec. Commission Géologique du Canada, Ottawa, Ontario, Compte Rendu du Ve Colloque de Géophysique Appliquée, 55e Congrès de l'ACFAS:101-127.
- BEN-MILOUD, K., M.K. SEGUIN & J. STEIN (in preparation). Watertable fluctuation study in a basin underlain by discontinuous permafrost, Northern Québec.
- FOURNIER, A., M. ALLARD & M.K. SEGUIN, 1987. Typologie morphogénétique des marelles du marais littoral de la baie de Kangiqsualujuaq, estuaire du George, Québec Nordique. *Géogr. phys. et Quat.*, 41:47-6.
- GAHÉ, É., M. ALLARD & M.K. SEGUIN, 1987. Géophysique et dynamique Holocène de plateau palsiques a Kangiqsualujuaq, Québec Nordique *Géogr. phys. Quat.*, 41:33-46.
- PAYETTE, S., 1983. The forest tundra and present treeline of the northern Quebec-Labrador. In *Tree-line Ecology. Proceedings of the Northern Quebec Tree-line Conference*, P. Morisset and S. Payette, Editors, *Nordicana*, 47:3-25.
- PARASNIS, D.S., 1972. *Principles of Applied Geophysics*. Chapman & Hall Ltd., London, p. 69-72.
- PILON, J.A., M. ALLARD & M.K. SEGUIN, (in press). Permafrost investigation with ground probing radar. Workshop on Ground Probing Radar, Ottawa, Canada.
- RIJKS WATERSTAAT, THE NETHERLANDS, 1969. Standard graphs for resistivity prospecting. European Ass. of Exploration Geophysicists.
- SEGUIN, M.K., M. ALLARD & É. GAHÉ, 1989. Surface and downhole geophysics for permafrost mapping in Ungava, Quebec. *Phys. Geogr.*, 10:201-232.
- SEGUIN, M.K., É. GAHÉ, M. ALLARD & K. BEN-MILOUD, 1989. Permafrost Geophysical investigation at the new airport site of Kangiqsualujuaq, Northern Quebec. In: *Proc. Fifth Inter. Conf. on Permafrost*, 2:980-987.
- SEGUIN, M.K. & M. ALLARD, 1987. La géophysique appliquée au pergélisol du Québec Nordique. *Géogr. Phys. Quat.*, 41:127-140.
- SCOTT, W.J., P.V. SELLMAN & J.A. HUNTER, 1978. Geophysics in the study of permafrost. In: *Proc. Third Inter. Conf. on Permafrost*, 2:93-115. TAYLOR, F.C., 1974. Reconnaissance geology of a part of the Precambrian shield, Northern Quebec and the Northwest Territories. Geological Survey of Canada, Paper 74-21, 9 pp. and map.
- TELFORD, W.M., L.P. GELDART, R.E. SHERIFF & D.A. KEYS, 1976. *Applied Geophysics*. Cambridge University Press, New York, 860 pp.
- ZODHY, A.A.R., 1975. Automatic interpretation of Schlumberger sounding curves using modified Dar Zarrouk functions. *U.S. Geol. Surv. Bull.*, 1313E:1-41.